Original Article
J Vet Sci 2015, 16(3), 297-306 · http://dx.doi.org/10.4142/jvs.2015.16.3.297

Cadmium induces apoptosis in primary rat osteoblasts through caspase and mitogen-activated protein kinase pathways

Hongyan Zhao†, Wei Liu†, Yi Wang, Nannan Dai, Jianhong Gu, Yan Yuan, Xuezhong Liu, Jianchun Bian, Zong-Ping Liu*

College of Veterinary Medicine, Yangzhou University, and Jiangsu Co-innovation Center for Prevention and Control of Important Animal Infectious Diseases and Zoonoses, Yangzhou 225009, China

Exposure to cadmium (Cd) induces apoptosis in osteoblasts (OBs); however, little information is available regarding the specific mechanisms of Cd-induced primary rat OB apoptosis. In this study, Cd reduced cell viability, damaged cell membranes and induced apoptosis in OBs. We observed decreased mitochondrial transmembrane potentials, ultrastructure collapse, enhanced caspase-3 activity, and increased concentrations of cleaved PARP, cleaved caspase-9 and cleaved caspase-3 following Cd treatment. Cd also increased the phosphorylation of p38-mitogen-activated protein kinase (MAPK), extracellular signal-regulated kinases (ERK)1/2 and c-jun N-terminal kinase (JNK) in OBs. Pretreatment with the caspase inhibitor, N-benzyloxycarbonyl-Val-Ala-Asp-fluoromethylketone, ERK1/2 inhibitor (U0126), p38 inhibitor (SB203580) and JNK inhibitor (SP600125) abrogated Cd-induced cell apoptosis. Furthermore, Cd-treated OBs exhibited signs of oxidative stress protection, including increased antioxidant enzymes superoxide dismutase and glutathione reductase levels and decreased formation of reactive oxygen species. Taken together, the results of our study clarified that Cd has direct cytotoxic effects on OBs, which are mediated by caspase- and MAPK pathways in Cd-induced apoptosis of OBs.

Keywords: apoptosis, cadmium, caspase, mitogen-activated protein kinase, osteoblasts

Introduction

Owing to worldwide demand for cadmium (Cd), approximately 30,000 tons of Cd are released into the environment each year [1]. This heavy metal is not degraded in the environment, which increases the risk of human exposure, with bone comprising an important target for Cd toxicity [2]. Exposure to high levels of Cd causes itai-itai disease, which is characterized by a combination of osteomalacia and osteoporosis [17]. It has been reported that low levels of Cd exposure could also give rise to bone injury by acting directly on osteoclasts (OBs) or affecting their function [11]. Previous reports have shown that Cd exposure can directly induce apoptotic OB death via the activation of caspases and mitogen-activated protein kinase (MAPK) [6,12]. Because apoptosis is recognized as an early cellular indicator of toxicity [35] and OBs are critical for bone formation, the interruption of apoptotic signaling cascades may give rise to bone diseases such as osteoporosis [36].

Oxidative stress usually occurs in cells exposed to Cd, and may overcome antioxidative defense systems, leading to cellular dysfunction [13]. Reactive oxygen species (ROS), an important indicator of oxidative stress, can occur in response to Cd exposure, resulting in damage to critical organelles, especially the mitochondria, eventually leading to apoptosis or necrosis [29,33]. Superoxide dismutase (SOD), catalase, and glutathione peroxidase and reductase (GR) are the major cellular defenses against ROS [38]. Accordingly, the relationship between redox homeostasis and apoptotic mechanisms of Cd-induced toxicity in OBs needs further investigation.

Studies have strongly suggested that oxidative mechanisms [14,20] and caspases [26,27], a family of cysteine-dependent aspartate-directed proteases, initiated and executed Cd-induced apoptosis. In addition, the involvement of other apoptotic pathways such as the MAPK-mediated pathway has been reported [16]. Nevertheless, these results have been contradictory, as experiments are commonly executed with high Cd concentrations for short

Received 20 Jun. 2014, Revised 5 Jan. 2015, Accepted 29 Jan. 2015
*Corresponding author: Tel: +86-13605273327; Fax: +86-514-87972218; E-mail: liuzongping@yzu.edu.cn
†The first two authors contributed equally to this work.
pISSN 1229-845X
eISSN 1976-555X

periods of time using a single cell type [32]. Therefore, we investigated whether standard exposure to Cd could induce apoptosis in OBs to clarify the role of oxidative stress, caspases, and MAPK activation in Cd-induced apoptosis.

Materials and Methods

Materials

Rhodamine 123 (Rh123), cadmium acetate (CdAc2), and Hoechst 33258 stain were purchased from Sigma Chemical (USA). Dulbecco's modified Eagle's medium (DMEM) and fetal bovine serum (FBS) were obtained from Gibco Laboratories (USA). Fluorescein isothiocyanate (FITC)-annexin V apoptosis detection kits were purchased from BD Biosciences Pharmingen (USA). Lactate dehydrogenase (LDH) and SOD assay kits were acquired from Jiancheng Bioengineering Institute (China). GR activity and caspase-3/CPP32 fluorometric assay kits were both obtained from BioVision Research Products (USA). Cell Counting Kit-8 (CCK8), ALP staining kits and bicinchoninic acid (BCA) protein assay kits were provided by the Beyotime Institute of Biotechnology (China). Anti-rat c-jun N-terminal kinase (JNK), P-JNK, extracellular signal-regulated kinase (ERK), P-ERK, p38, P-p38, β-actin, cleaved poly (ADP-ribose) polymerase (PARP), cleaved caspase-9, cleaved caspase-3, Bax, Bcl-2, and horseradish peroxidase (HRP)-conjugated goat anti-rabbit IgG antibodies were obtained from Cell Signaling Technology (USA).

Cell culture

Sprague-Dawley rats were purchased from the Laboratory Animal Center of Jiangsu University. OBs were obtained by sequential enzyme digestion of calvarial bones from 18–19 day gestational rats. Briefly, the clean calvariae were gently incubated at 37°C for 10 min with 0.25% (w/v) trypsin in phosphate-buffered saline (PBS), cut into slices, and incubated at 37°C for 40 min with 0.1% collagenase followed by the collection of cells. The cells were resuspended in DMEM supplemented with 10% FBS, 2 mM L-glutamine, 100 U/mL penicillin, and 100 μg/mL streptomycin, then cultured at 37°C in 95% humidified air containing 5% CO_2. During culture, the medium was replaced every 2 days, and the cells were passaged. Cells from passage two or three were used for all experiments. The phenotype was identified by alkaline phosphatase (ALP) staining using an ALP staining kit.

Cell suspensions (2×10^5 cells/mL) were seeded in 6-, 24- or 96-well flat-bottomed plates. When the cells reached 70 to 80% confluence, they were exposed to increasing concentrations (0–20 μM) of Cd in the presence and absence of an ion channel blocker for 0 to 48 h.

Cell viability assays

After Cd treatment, cell viability was evaluated using CCK8. All experimental procedures were executed according to the manufacturer's instructions, and water-soluble tetrazolium (WST) absorbance was measured at 450 nm with a basic Sunrise ELISA reader (Tecan, Austria). Cell viability was expressed as the proportion of optical density (OD) to the control.

Measurement of LDH, SOD, and GR activity

Cd-treated cells were lysed with cell lysis solution (0.1 M Tris-HCl and 0.1% Triton-100), after which they were centrifuged at 2,000 × g and 4°C for 5 min to obtain the supernatant. The activities of LDH, SOD, and GR were subsequently determined according to the instructions of LDH, SOD and GR activity assay kits described in the Materials part, respectively. The LDH result was expressed as the leakage proportion to the total level of LDH.

Measurement of ROS and mitochondrial transmembrane potential

To detect ROS and mitochondrial transmembrane potential (MMP), harvested cells were incubated with dichloro-dihydro-fluorescein diacetate (DCFH-DA; final concentration, 10 μmol/L) and rhodamine (Rh)-123 (final concentration, 10 mg/L), respectively, in the dark at 37°C for 30 min, washed twice, and resuspended in PBS. Assay results were calculated by the fluorescence intensity (FL-1, 530 nm) of 10,000 cells using a FACSAria flow cytometer (Becton, Dickinson and Company, USA).

Transmission electron microscopy

Following Cd treatment, internal cellular structures were examined using a PHILIPS CM-120 transmission electron microscope. Briefly, cells were fixed with 2.5% glutaraldehyde at 4°C for 24 h and embedded in agar. The samples were then treated with 1% osmium tetroxide for 2 h and dehydrated using a graded acetone series, after which they were placed in a pure acetone and Epon 812 epoxy solution for 30 min and embedded in Epon 812 epoxy at 60°C for 48 h. Ultrathin (70 nm) sections were cut with a diamond knife and stained with lead and uranium.

Hoechst 33258 staining

Cells were fixed in 4% formaldehyde for 10 min, incubated with 5 μg/mL Hoechst 33258 at 37°C for 15 min, then washed twice with PBS. Stained cells were immediately examined under a fluorescence microscope (Nikon, Japan) at an excitation wavelength of 330 to 380 nm using 450 to 490 nm filters.

FITC-annexin V/propidium iodide staining

Cells were suspended in 100 μL of 1× binding buffer containing 5 μL FITC-annexin V and 5 μL propidium iodide (PI) dye solution. After incubation at room temperature in the

dark for 15 min, 400 μL binding buffer was added. The scatter parameters of the cells were subsequently analyzed using a flow cytometer at an excitation wavelength of 488 nm and emission wavelength of 605 nm. The apoptosis percentage was summed for both primary apoptosis (annexin V^+/PI^-) and late apoptosis (annexin V^+/PI^+).

Measurement of caspase-3 activity

After incubation with Cd, caspase-3 activity was assessed by a caspase-3/CPP32 fluorometric assay kit following the manufacturer's instructions. Data were expressed as the fold-change in caspase-3 activity compared with non-treated controls (n = 3).

Western blot analysis

After incubation with Cd, cells were washed twice with PBS and lysed in radioimmunoprecipitation assay (RIPA) lysis buffer for 30 min at 4°C. Following sonication and centrifugation, the protein concentration of the cells was measured using a BCA protein assay kit according to the manufacturer's instructions. The protein samples were separated using 10% sodium dodecyl sulfate polyacrylamide gel electrophoresis (SDS-PAGE), transferred to nitrocellulose (Pall Corporation, USA), and then incubated overnight with the primary antibodies (rabbit anti-rat antibodies to P-p38, p38, P-ERK, ERK, P-JNK, JNK, cleaved PARP, cleaved caspase-9, cleaved caspase-3, Bax, and Bcl-2 at dilutions of 1 : 1000; anti-β-actin antibody was used at a dilution of 1 : 5000) at 4°C, followed by incubation with HRP-conjugated goat anti-rabbit IgG for 2 h at 1 : 5000. Proteins were visualized using enhanced chemiluminescence detection reagents. The band intensity was determined by a gel image analysis system (Bio-Rad Laboratories, USA) and normalized with β-actin.

Statistical analysis

The results reported are the mean and standard deviation (SDs) of three independent experiments, each performed in duplicate or triplicate. Statistical comparisons were made using one-way analysis of variance (ANOVA; Student's *t*-test) after ascertaining the homogeneity of variance between treatments. A $p < 0.05$ was considered statistically significant.

Results

Cd altered cell viability, LDH, antioxidant enzymatic activity, ROS, mitochondrial membrane potential, and the ultrastructure of OBs

Cd decreased cell viability in a concentration-dependent manner (0.5–20 μM; panel A in Fig. 1). Cell viability significantly decreased after treatment with 2 μM Cd for all time-points, and 45% of viable cells remained at the 24 h time-point, indicating a median inhibitory concentration (IC50) value of approximately 2 μM. Therefore, we selected 1, 2, and 5 μM Cd for subsequent experiments. The degree of cellular injury caused by Cd was estimated by the leakage of LDH enzymes. The cell number varied between plates; therefore, we compared the injury levels using the leakage ratio of experimental LDH to the corresponding maximum LDH. We observed a dose-dependent increase in this ratio, and approximately 50% of cells exhibited ruptured membranes after treatment with 2 μM Cd for 24 h (panel B in Fig. 1).

To assess the intracellular antioxidant status, SOD and GR activity were evaluated in Cd-treated OBs (panel C in Fig. 1). Cd treatment significantly increased SOD activity in a dose-dependent manner. GR activity was higher in cells treated with 1 μM Cd than in the controls. With further increases in Cd concentration, GR activity decreased in a concentration-dependent manner. Intracellular ROS were measured in OBs (panel D in Fig. 1). Cd treatment produced a dose-dependent decrease in ROS at 12 and 24 h, while DCF fluorescence was remarkably decreased compared with that in the control group at additional time-points.

MMP increased after 0.75 h of 1 μM Cd treatment; however, 5 μM Cd for 1.5 h led to significantly decreased MMP (panel E in Fig. 1). We observed a significant MMP reduction at 24 h at 1 μM, while 5 μM Cd reduced the mitochondrial potential by 35%. Control cells exhibited oval mitochondria with well-defined transversal cristae (panel F1 in Fig. 1). However, after treatment with 1 μM Cd for 24 h, the OBs exhibited mitochondrial swelling and vague cristae (panel F2 in Fig. 1). As the Cd dose increased, OBs showed disappearance of mitochondrial cristae and cytoplasmic vacuolation (panels F3-4 in Fig. 1).

Cd triggers apoptosis in OBs

The nuclei of apoptotic cells showed an increase in fluorescence and typical apoptotic bodies (panels A and B in Fig. 2). The apoptotic rate increased in a dose-dependent manner at both 12 and 24 h (panel C in Fig. 2). Treatment with 2 μM Cd for 24 h doubled the number of apoptotic cells compared to the number in the control group.

The expression levels of Bax and Bcl-2 were investigated in OBs. Treatment with Cd for 24 h upregulated the expression of Bax, but downregulated the expression of Bcl-2 in a dose-dependent manner. The ratio of Bax/Bcl-2 increased by approximately 2.96-fold compared to the control (panels D and E in Fig. 2).

Involvement of caspase-dependent pathways in Cd-mediated cell apoptosis

Exposure to 2 μM Cd led to a significant time-dependent increase in caspase-3 activity compared with the control (panel A in Fig. 3). In addition, the stimulation of caspase-3 activity was concentration-dependent (panel B in Fig. 3). Furthermore, pretreatment of cells with 50 μM of the pan-caspase inhibitor,

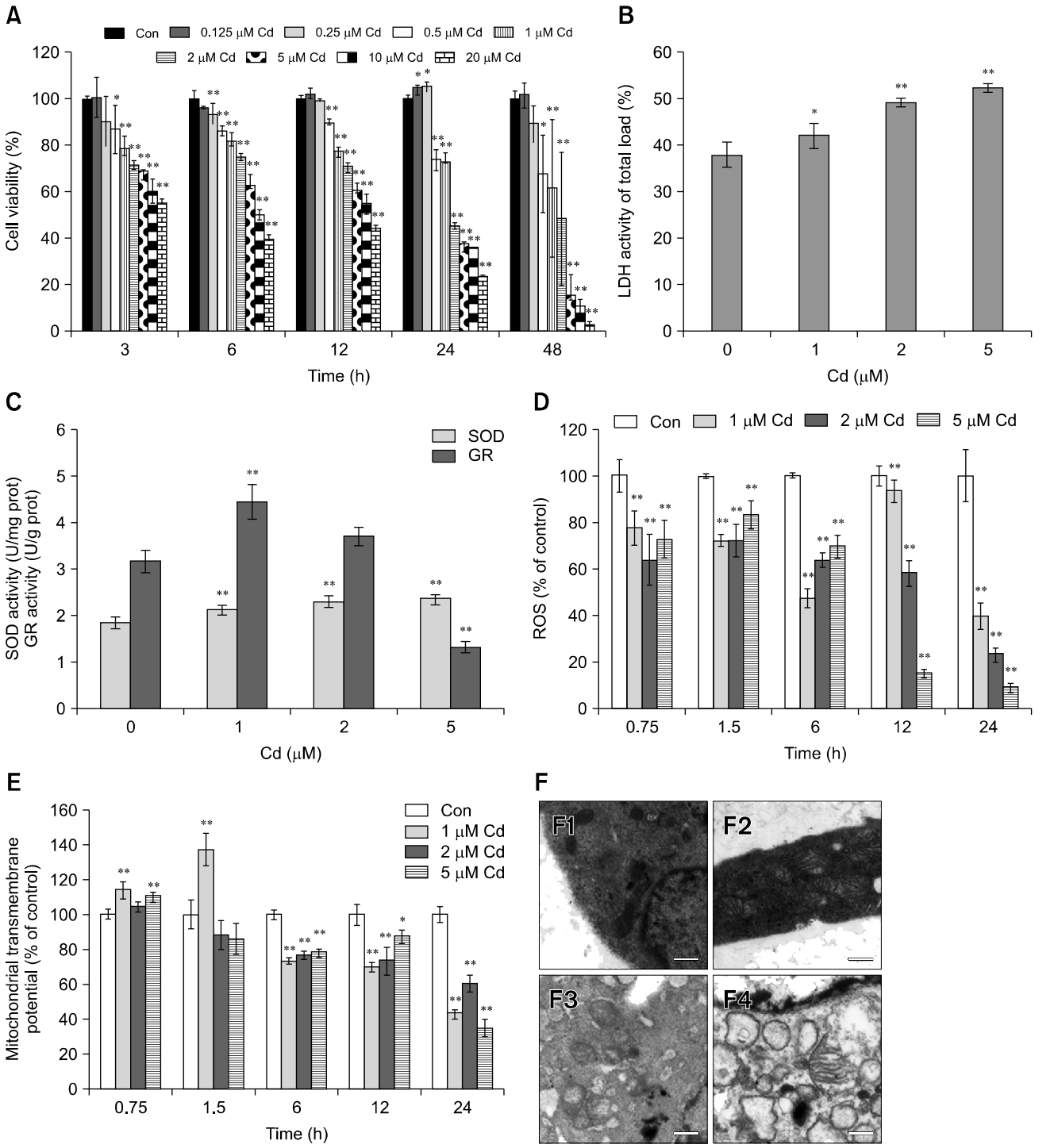

Fig. 1. Cadmium (Cd) altered cell viability, lactate dehydrogenase (LDH), antioxidant enzymatic activity, reactive oxygen species (ROS), mitochondrial membrane potential and ultrastructure in osteoblasts (OBs). (A) OBs were treated with 0–20 μM Cd, and cell viability was assessed at 3 to 48 h. (B and C) OBs were treated with 0–5 μM Cd for 24 h, and LDH, SOD, and glutathione reductase (GR) activities were determined. (D and E) Cells were exposed to 0–5 μM Cd for 0.75 to 24 h. Intracellular ROS production and mitochondrial transmembrane potential (MMP) were measured, and the results are presented as the mean fluorescence intensity (MFI) relative to the control group (100%). Data are presented as the mean and SDs of three independent experiments, each performed in triplicate. Significant differences are indicated by $*p < 0.05$ and $**p < 0.01$ relative to the control. (F) Ultrastructural morphology of OBs (5,200× magnification) after treatment with 0, 1, 2, and 5 μM Cd (F1–4) for 24 h.

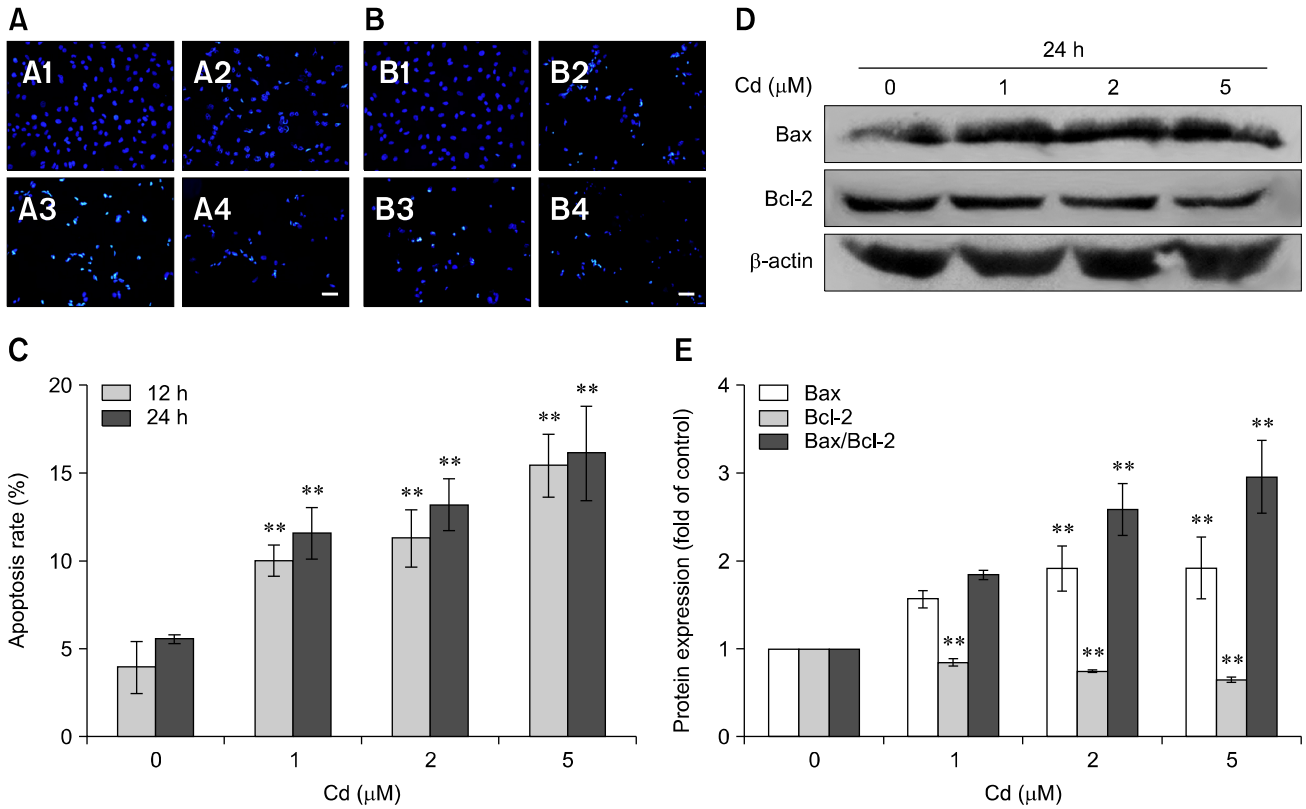

Fig. 2. Cd triggers apoptosis in OBs. (A and B) Cell nuclei as observed under fluorescence microscopy. Cells were exposed to 0 (A1 and B1), 1 (A2 and B2), 2 (A3 and B3), and 5 (A4 and B4) μM Cd for 12 h (A) and 24 h (B). Scale bars = 20 μm (A and B). (C) Flow cytometric analysis of cells showed an increased apoptotic rate in a dose-dependent manner. (D) The expression levels of Bax and Bcl-2 were assessed by western blot analysis, while β-actin was probed as a protein loading control. (E) Densitometry analysis of Bax, Bcl-2 and the Bax/Bcl-2 ratio. All data were expressed as the mean and SDs (n = 3). $^{**}p < 0.01$ compared with the control group.

N-benzyloxycarbonyl-Val-Ala-Asp-fluoromethylketone (Z-VAD-fmk), 1 h before the addition of Cd inhibited the Cd-induced reduction in cell viability (panel C in Fig. 3) and Cd-mediated cell apoptosis (panel D in Fig. 3).

Western blot analysis (panel E in Fig. 3) showed that Cd exposure significantly increased the concentration of cleaved PARP, cleaved caspase-9 and cleaved caspase-3, which suggested the involvement of mitochondria-dependent signaling cascades during the Cd-induced apoptosis of OBs.

Involvement of MAPK signaling in Cd-induced apoptosis

Cd significantly stimulated the activity of p38 in the early period (from 2 to 6 h) after 1 h of Cd treatment in a time-dependent manner. We observed intense stimulation of ERK1/2 phosphorylation after Cd treatment for 2 h that increased until 5 h (panels A and C in Fig. 4). Cd at 2 μM also stimulated the phosphorylation of JNK early at 1 h, and these effects lasted for 6 h. These results suggest that Cd activates p38, ERK1/2 and JNK.

We next investigated the role that MAPK signaling played in Cd-induced apoptosis. The results showed that it significantly attenuated the expression of apoptosis-related protein Bax/Bcl2 when cells were pre-incubated with 10 μM SB203580, SP600125, and U0126 for 30 min before treatment with 2 μM Cd relative to cells treated with Cd alone (panels B and D in Fig. 4). These results suggest that MAPK signaling may play an important role in Cd-induced apoptosis.

Discussion

Cell proliferation and differentiation can be affected by Cd, and recent studies have demonstrated that Cd can cause cell apoptosis [4,19]. Furthermore, Cd acts directly on the activity and metabolism of bone cells and the process of mineralization [10,11]. However, the underlying mechanisms responsible for this effect are unclear. Therefore, our study investigated the toxicological effects and underlying mechanisms of Cd-induced primary rat OB injuries, especially with regards to apoptosis.

Oxidative stress is believed to participate in the early processes of proximal tubular kidney damage induced by subtoxic doses of Cd [33], causing pancreatic beta-cell death [8] and the apoptosis of H4-II-E-C3 rat liver-derived cell lines [8]. However,

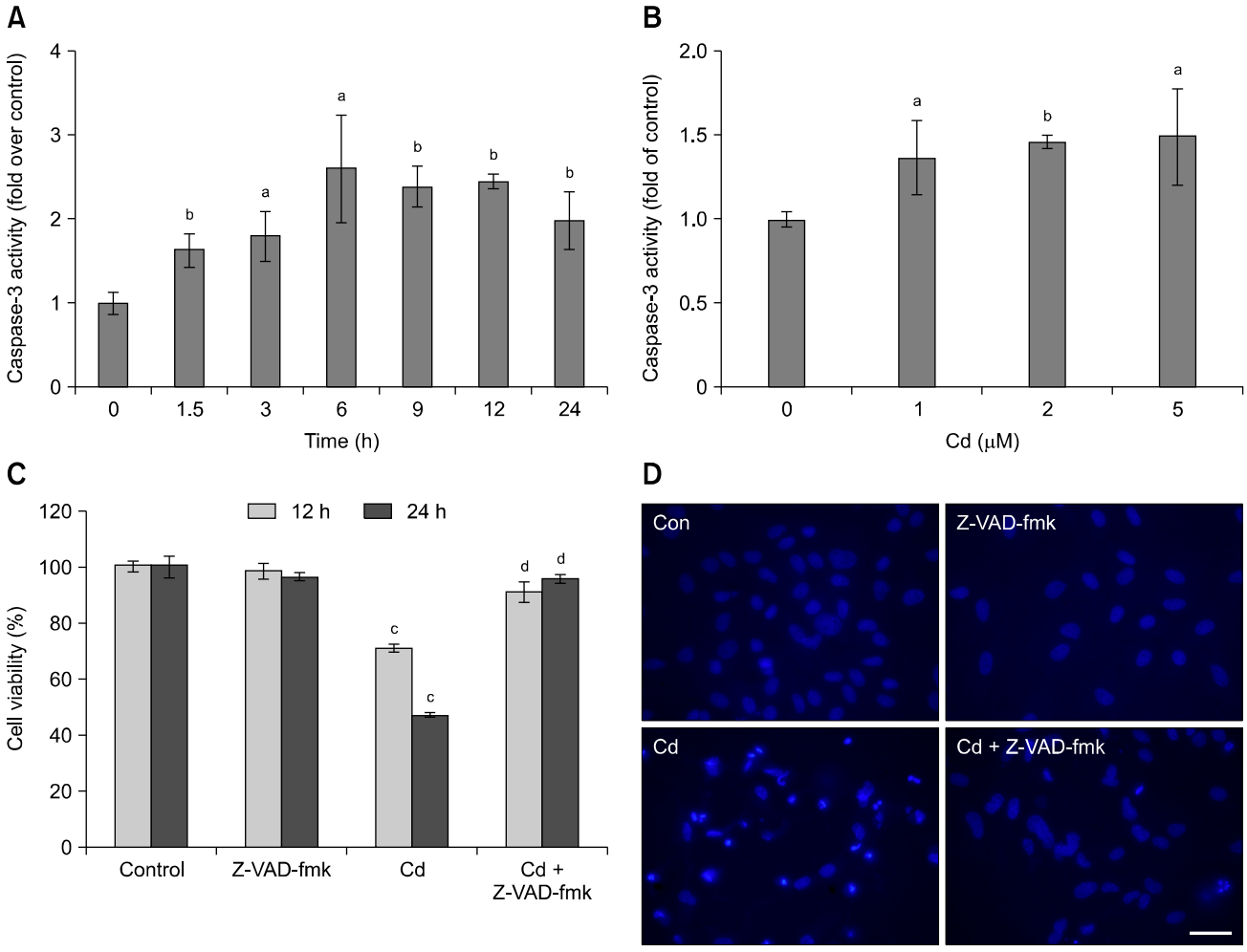

Fig. 3. Caspase activation is partially associated with Cd-induced apoptosis. (A) Time course of Cd-induced (2 μM) changes in caspase-3 activity. Data are expressed as the x-fold change over control values estimated in untreated cells. (B) Cd (0, 1, 2, 5 μM) stimulated caspase-3 activity. Data are expressed as the x-fold change over control values as estimated in untreated cells. (C) Cells were exposed to the indicated concentrations of Cd in the presence or absence of 50 μM z-VAD-fmk for 12 and 24 h, and cell viability was analyzed. (D) Morphological changes in OB nuclei after 2 μM Cd treatment in the presence or absence of 50 μM z-VAD-fmk for 24 h. Scale bar = 20 μm. (E) Cd increased the protein expression levels of cleaved PARP, cleaved caspase-9 and cleaved caspase-3. The intensity of each band was quantified by densitometry. The protein expression from the control group was designated as 1, while that of the other groups were expressed as fold changes compared to the control. Data are presented as the means and SDs of three independent experiments, each performed in triplicate. Significant differences are indicated by $^{a}p < 0.05$ and $^{b}p < 0.01$ relative to the control, and $^{c}p < 0.05$ and $^{d}p < 0.01$ compared with the Cd group.

in this study, we observed a decrease in ROS generation in OBs treated with Cd, which was in contrast to the findings of many other studies [26,40]. The increase in antioxidant enzymes, SOD and GR, might have contributed to the decrease in ROS generation; however, further investigation was necessary to explore the exact mechanisms of the decrease in ROS. Cell protection and clearance are the two main responses of cells exposed to toxic agents. A study by Regunathan et al. showed that bone cells exposed to Cd had increased levels of metallothionein (MT) and transferrin receptor synthesis [30]. Furthermore, several other studies showed that Cd increased MT gene expression in both osteocytes and rat bone tissue [2,23]. It has also been reported that the OB transcriptional factor, RUNX2, a target for heavy metal-induced osteotoxicity, is involved in protective responses against osteoporosis in postmenopausal women. Genes that participate in cell death, repair and mammalian cell cycling can be activated by redox stress and induce apoptosis or long-term protection strategies against oxidative stress [32]. In chronically Cd-poisoned cells, the production of ROS was found to decrease in accordance with aberrant gene expression levels to enable cells become tolerant to Cd [20].

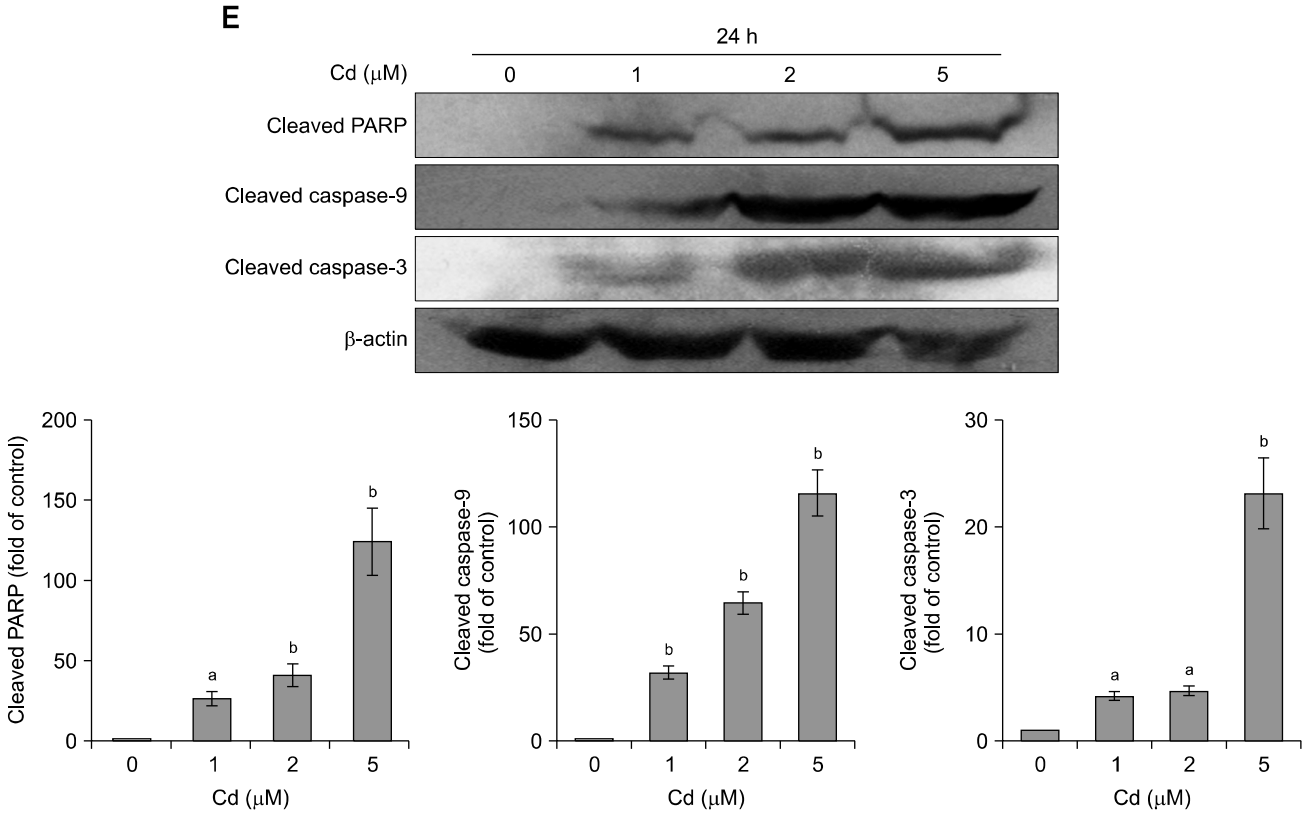

Fig. 3. Continued.

Bcl-2 or Bcl-xL expression regulates the exchange of mitochondrial adenine nucleotide, which is associated with apoptosis [34]. The functions of the two proteins are completely opposite. Bcl-2 possesses anti-apoptotic effects by maintaining mitochondrial homeostasis, while Bax activates caspase signaling and induces apoptosis by downregulating mitochondrial permeability [24]. The ratio of Bax/Bcl-2 is generally one of the most important indicators of apoptosis. Our results demonstrated a higher Bax/Bcl-2 ratio in Cd-treated cells than untreated control cells. In addition, the activation of caspase signaling is another vital marker of mitochondria-caused apoptosis. Caspases, a family of cysteine-dependent aspartate-directed proteases, participate in the initiation and execution of apoptosis [7]. Among various caspases, the main effector is caspase-3, which plays a critical role in inducing characteristic apoptotic changes and is closely associated with many other apoptotic mediators, such as PARP, cytochrome c and caspase-9 [28]. Caspase-9 is an initiator caspase that activates downstream caspases, such as caspases-3, -6 and -7 [37]. Our results demonstrated that Cd-induced apoptosis in OBs involves activation of the cleavage of PARP, caspase-9 and caspase-3. Pretreatment of the cells with a broad spectrum inhibitor, Z-VAD-fmk, attenuated Cd-induced cell apoptosis, revealing that caspase-dependent pathways are partially connected to Cd-induced cell apoptosis.

MAPKs, a family of protein-serine/threonine kinases (including p38-MAPK, JNK, and ERK), regulate cell survival, proliferation, differentiation and death [5]. p38-MAPK and JNK are involved in cell apoptosis by participating in the cellular response to stress, while cell survival is usually regulated by ERK with a short-term period of activation. However, it is still unclear how MAPKs regulate OB apoptosis. Hence, our results extend the findings of previous studies to OBs derived from 18−19 day gestational Sprague-Dawley rats. Our findings showed that 2 μM Cd significantly stimulated activation of the ERK pathway soon after treatment for 2 h. This observation was consistent with previous findings that Cd poisoning leads to activation of the ERK pathway and ultimately apoptosis in CCRF-CEM human T lymphoblastoid cells [15], mesangial cells [39], and Saos-2 OBs [3]. Martin *et al*. [22] demonstrated that low dose Cd resulted in unconventional ERK-sustained phosphorylation in several cell types, which subsequently led to death signaling. Lag *et al*. [18] reported that, although Cd exposure promptly increased the phosphorylation of p38 MAPK, ERK1/2, and JNK, only p38 inhibitor reduced Cd-induced apoptosis. These findings suggested that p38 is involved in apoptosis of lung cells, which is in accordance with the findings of Stinson *et al*. [31], who reported that Cd-induced caspase-independent apoptosis of mesangial cells is associated with activated p38

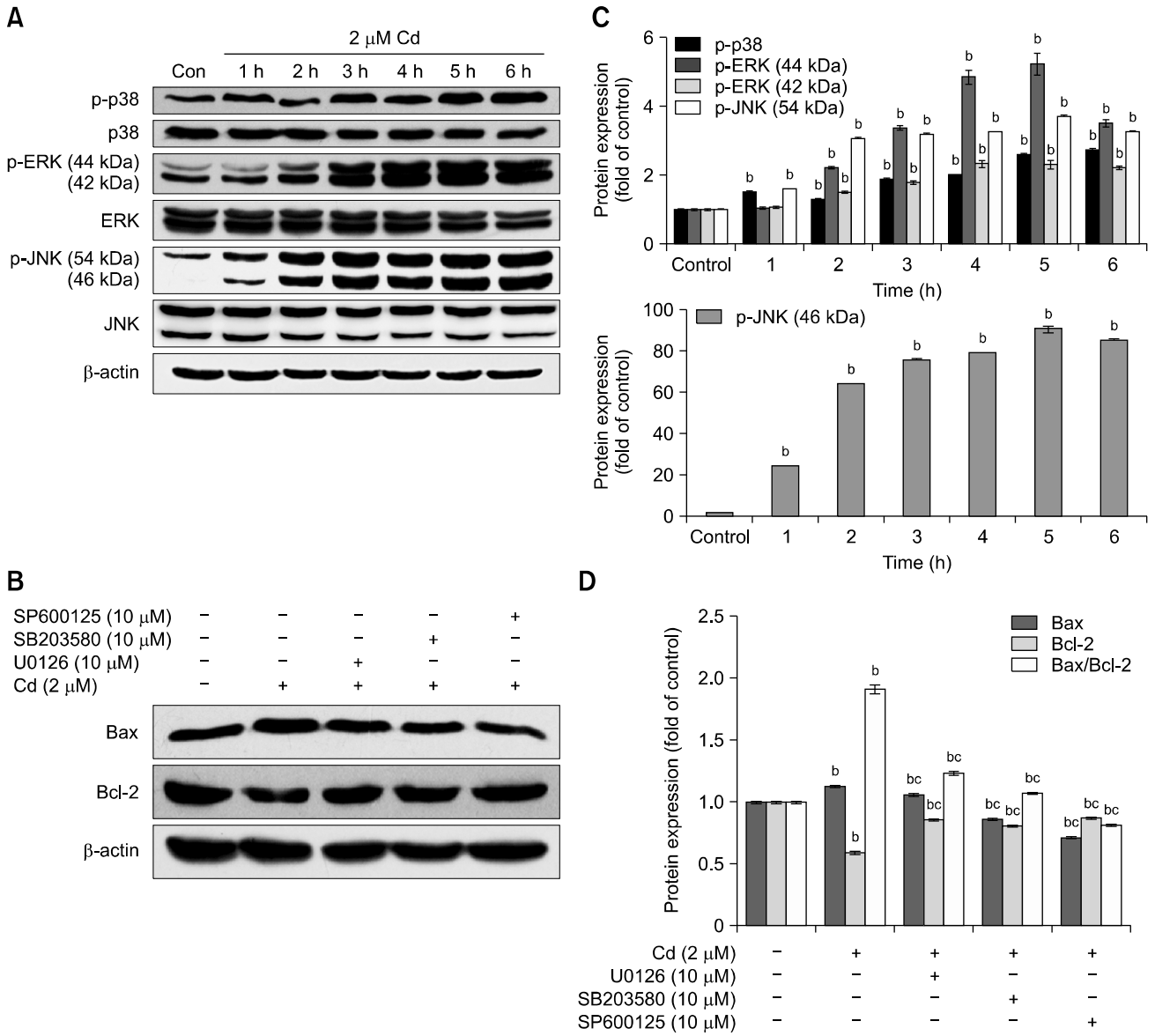

Fig. 4. The involvement of MAPK signaling in Cd-induced apoptosis. Cell lysates analyzed by western blot with the indicated antibodies. The β-actin protein level was used as a loading control. (A) Cells were cultured with 2 μM Cd for 1 to 6 h. (B) OBs were pre-incubated with 10 μM SB203580, SP600125, and U0126 for 30 min, followed by incubation with 2 μM Cd for 12 h. (C and D) The amount of phosphorylated protein was quantified by densitometry and corrected for sample loading based on the density of the β-actin band. The results are expressed as the fold changes relative to the control lane. Each blot is representative of at least three replicate experiments. $^{a}p < 0.05$, $^{b}p < 0.01$ relative to the control and $^{c}p < 0.01$ relative to the Cd-treated group.

MAPK [21]. Papadakis *et al*. [25] found that indicators of apoptosis, including the activation of Bax, caspase activity and DNA fragmentation, were absent from JNK-deficient fibroblasts, suggesting that JNK mediates fibroblast apoptosis. Furthermore, ROS formation is associated with the activation of JNK signaling via a Ca^{2+}-dependent pathway [9,15]. In this study, we demonstrated that 2 μM Cd significantly enhanced the phosphorylation levels of p38-MAPK and ERK1/2, but not JNK. Furthermore, the pretreatment of cells with a specific ERK1/2 inhibitor (U0126), p38 inhibitor (SB203580) and JNK inhibitor (SP600125) reduced the ratio of Bax/Bcl-2 relative to the Cd-treated group. These results indicate that p38, ERK and JNK are involved in Cd-induced apoptosis in OBs.

Acknowledgments

This work was supported by grants from the National Natural Science Foundation of China (nos. 31302058 and 31172373),

the Priority Academic Program Development of Jiangsu Higher Education Institutions, the Graduate Innovation Project of Jiangsu Province and the Specialized Research Fund for the Doctoral Program of Higher Education (no. 20113250110003), China.

Conflict of Interest

There is no conflicts of interest.

References

1. **Agency for Toxic Substance and Disease Registry (ATSDR).** Toxicological profile for Cadmium. Department of Health and Human Services, Public Health Service (US). Atlanta, 2005.
2. **Angle CR, Thomas DJ, Swanson SA.** Osteotoxicity of cadmium and lead in HOS TE 85 and ROS 17/2.8 cells: relation to metallothionein induction and mitochondrial binding. Biometals 1993, **6**, 179-184.
3. **Arbon KS, Christensen CM, Harvey WA, Heggland SJ.** Cadmium exposure activates the ERK signaling pathway leading to altered osteoblast gene expression and apoptotic death in Saos-2 cells. Food Chem Toxicol 2012, **50**, 198-205.
4. **Bertin G, Averbeck D.** Cadmium: cellular effects, modifications of biomolecules, modulation of DNA repair and genotoxic consequences (a review). Biochimie 2006, **88**, 1549-1559.
5. **Boutros T, Chevet E, Metrakos P.** Mitogen-activated protein (MAP) kinase/MAP kinase phosphatase regulation: roles in cell growth, death, and cancer. Pharmacol Rev 2008, **60**, 261-310.
6. **Brama M, Politi L, Santini P, Migliaccio S, Scandurra R.** Cadmium-induced apoptosis and necrosis in human osteoblasts: role of caspases and mitogen-activated protein kinases pathways. J Endocrinol Invest 2012, **35**, 198-208.
7. **Budihardjo I, Oliver H, Lutter M, Luo X, Wang X.** Biochemical pathways of caspase activation during apoptosis. Annu Rev Cell Dev Biol 1999, **15**, 269-290.
8. **Chang KC, Hsu CC, Liu SH, Su CC, Yen CC, Lee MJ, Chen KL, Ho TJ, Hung DZ, Wu CC, Lu TH, Su YC, Chen YW, Huang CF.** Cadmium induces apoptosis in pancreatic β-cells through a mitochondria-dependent pathway: the role of oxidative stress-mediated c-Jun N-terminal kinase activation. PLoS One 2013, **8**, 54374.
9. **Chen L, Liu L, Huang S.** Cadmium activates the mitogen-activated protein kinase (MAPK) pathway via induction of reactive oxygen species and inhibition of protein phosphatases 2A and 5. Free Radic Biol Med 2008, **45**, 1035-1044.
10. **Chen X, Zhu G, Gu S, Jin T, Shao C.** Effects of cadmium on osteoblasts and osteoclasts *in vitro*. Environ Toxicol Pharmacol 2009, **28**, 232-236.
11. **Chen X, Zhu G, Jin T, Zhou Z, Gu S, Qiu J, Xiao H.** Cadmium stimulates the osteoclastic differentiation of RAW264.7 cells in presence of osteoblasts. Biol Trace Elem Res 2012, **146**, 349-353.
12. **Coonse KG, Coonts AJ, Morrison EV, Heggland SJ.** Cadmium induces apoptosis in the human osteoblast-like cell line Saos-2. J Toxicol Environ Health A 2007, **70**, 575-581.
13. **Cuypers A, Plusquin M, Remans T, Jozefczak M, Keunen E, Gielen H, Opdenakker K, Nair AR, Munters E, Artois TJ, Nawrot T, Vangronsveld J, Smeets K.** Cadmium stress: an oxidative challenge. Biometals 2010, **23**, 927-940.
14. **Ikediobi CO, Badisa VL, Ayuk-Takem LT, Latinwo LM, West J.** Response of antioxidant enzymes and redox metabolites to cadmium-induced oxidative stress in CRL-1439 normal rat liver cells. Int J Mol Med 2004, **14**, 87-92.
15. **Iryo Y, Matsuoka M, Wispriyono B, Sugiura T, Igisu H.** Involvement of the extracellular signal-regulated protein kinase (ERK) pathway in the induction of apoptosis by cadmium chloride in CCRF-CEM cells. Biochem Pharmacol 2000, **60**, 1875-1882.
16. **Junttila MR, Li SP, Westermarck J.** Phosphatase-mediated crosstalk between MAPK signaling pathways in the regulation of cell survival. FASEB J 2008, **22**, 954-965.
17. **Kjellström T.** Mechanism and epidemiology of bone effects of cadmium. IARC Sci Publ 1992, 301-310.
18. **Låg M, Refsnes M, Lilleaas EM, Holme JA, Becher R, Schwarze PE.** Role of mitogen activated protein kinases and protein kinase C in cadmium-induced apoptosis of primary epithelial lung cells. Toxicology 2005, **211**, 253-264.
19. **Liu J, Kadiiska MB, Corton JC, Qu W, Waalkes MP, Mason RP, Liu Y, Klaassen CD.** Acute cadmium exposure induces stress-related gene expression in wild-type and metallothionein-I/II-null mice. Free Radic Biol Med 2002, **32**, 525-535.
20. **Liu J, Qu W, Kadiiska MB.** Role of oxidative stress in cadmium toxicity and carcinogenesis. Toxicol Appl Pharmacol 2009, **238**, 209-214.
21. **Liu Y, Templeton DM.** Initiation of caspase-independent death in mouse mesangial cells by Cd^{2+}: involvement of p38 kinase and CaMK-II. J Cell Physiol 2008, **217**, 307-318.
22. **Martin P, Poggi MC, Chambard JC, Boulukos KE, Pognonec P.** Low dose cadmium poisoning results in sustained ERK phosphorylation and caspase activation. Biochem Biophys Res Commun 2006, **350**, 803-807.
23. **Oda N, Sogawa CA, Sogawa N, Onodera K, Furuta H, Yamamoto T.** Metallothionein expression and localization in rat bone tissue after cadmium injection. Toxicol Lett 2001, **123**, 143-150.
24. **Ola MS, Nawaz M, Ahsan H.** Role of Bcl-2 family proteins and caspases in the regulation of apoptosis. Mol Cell Biochem 2011, **351**, 41-58.
25. **Papadakis ES, Finegan KG, Wang X, Robinson AC, Guo C, Kayahara M, Tournier C.** The regulation of Bax by c-Jun N-terminal protein kinase (JNK) is a prerequisite to the mitochondrial-induced apoptotic pathway. FEBS Lett 2006, **580**, 1320-1326.
26. **Pathak N, Mitra S, Khandelwal S.** Cadmium induces thymocyte apoptosis via caspase-dependent and caspase-independent pathways. J Biochem Mol Toxicol 2013, **27**, 193-203.
27. **Petanidis S, Hadzopoulou-Cladaras M, Salifoglou A.** Cadmium

modulates H-ras expression and caspase-3 apoptotic cell death in breast cancer epithelial MCF-7 cells. J Inorg Biochem 2013, **121**, 100-107.
28. **Porter AG, Jänicke RU.** Emerging roles of caspase-3 in apoptosis. Cell Death Differ 1999, **6**, 99-104.
29. **Pourahmad J, O'Brien PJ, Jokar F, Daraei B.** Carcinogenic metal induced sites of reactive oxygen species formation in hepatocytes. Toxicol In Vitro 2003, **17**, 803-810.
30. **Regunathan A, Glesne DA, Wilson AK, Song J, Nicolae D, Flores T, Bhattacharyya MH.** Microarray analysis of changes in bone cell gene expression early after cadmium gavage in mice. Toxicol Appl Pharmacol 2003, **191**, 272-293.
31. **Stinson LJ, Darmon AJ, Dagnino L, D'Souza SJ.** Delayed apoptosis post-cadmium injury in renal proximal tubule epithelial cells. Am J Nephrol 2003, **23**, 27-37.
32. **Thévenod F.** Cadmium and cellular signaling cascades: to be or not to be? Toxicol Appl Pharmacol 2009, **238**, 221-239.
33. **Thijssen S, Cuypers A, Maringwa J, Smeets K, Horemans N, Lambrichts I, Van Kerkhove E.** Low cadmium exposure triggers a biphasic oxidative stress response in mice kidneys. Toxicology 2007, **236**, 29-41.
34. **Vander Heiden MG, Chandel NS, Li XX, Schumacker PT, Colombini M, Thompson CB.** Outer mitochondrial membrane permeability can regulate coupled respiration and cell survival. Proc Natl Acad Sci U S A 2000, **97**, 4666-4671.
35. **Weber LP, Kiparissis Y, Hwang GS, Niimi AJ, Janz DM, Metcalfe CD.** Increased cellular apoptosis after chronic aqueous exposure to nonylphenol and quercetin in adult medaka (*Oryzias latipes*). Comp Biochem Physiol C Toxicol Pharmacol 2002, **131**, 51-59.
36. **Xing L, Boyce BF.** Regulation of apoptosis in osteoclasts and osteoblastic cells. Biochem Biophys Res Commun 2005, **328**, 709-720.
37. **Xu J, Zhou M, Ouyang J, Wang J, Zhang Q, Xu Y, Xu Y, Zhang Q, Xu X, Zeng H.** Gambogic acid induces mitochondria-dependent apoptosis by modulation of Bcl-2 and Bax in mantle cell lymphoma JeKo-1 cells. Chin J Cancer Res 2013, **25**, 183-191.
38. **Yamamoto T, Hsu S, Lewis J, Wataha J, Dickinson D, Singh B, Bollag WB, Lockwood P, Ueta E, Osaki T, Schuster G.** Green tea polyphenol causes differential oxidative environments in tumor versus normal epithelial cells. J Pharmacol Exp Ther 2003, **307**, 230-236.
39. **Yang LY, Wu KH, Chiu WT, Wang SH, Shih CM.** The cadmium-induced death of mesangial cells results in nephrotoxicity. Autophagy 2009, **5**, 571-572.
40. **Zhang Y, Jiang C, Wang J, Yuan Y, Gu J, Bian J, Liu X, Liu Z.** Oxidative stress and mitogen-activated protein kinase pathways involved in cadmium-induced BRL 3A cell apoptosis. Oxid Med Cell Longev 2013, **2013**, 516051.